spectral height decreases with practically a constant rate. The medium-dose samples exhibit the same rate, which is larger than the rate for the light-dose sample. From T_2 to T_3, however, a larger rate of decrease sets in. The new rate is larger, for increasing neutron dose. Above T_3, the spectral height appears to approach gradually a limiting value.

In the case of heavy-dose samples, the width, shape, and height of EPR spectra remain unchanged, and appear to be insensitive to the varying temperature below 233°C. An extension of the work into the temperature range above 233°C is currently being undertaken.

The two-center model and the assumption that the activation energy of F centers is a monotonically decreasing function of F-center concentration have been adopted for explaining most of the observed results. The approach has been found to be successful for explaining the observed behavior of EPR spectra of medium-dose samples at temperatures above T_1 and that of heavy-dose samples up to 233°C. It is possible for the model to provide an explanation for the behavior of medium-dose and light-dose samples below T_1, and the effect of heat treatments on the hyperfine structure of F centers.

However, the model seems to encounter some difficulties when it is applied to the case of the broadening of EPR spectra of light-dose samples above T_1. For this case, an additional assumption has been made: Annihilation and/or possibly conversion of cluster centers into F centers takes place through thermal dissolution. This assumption is very speculative in nature, but seems to be necessary in order to sustain the two-center model. Accordingly, further tests and consolidation of these assumptions seem to be necessary. A series of optical absorption studies of the samples have already been initiated for this purpose.

PHYSICAL REVIEW VOLUME 137, NUMBER 4A 15 FEBRUARY 1965

Stored-Energy Release Below 80°K in Deuteron-Irradiated Copper*

T. G. NILAN† AND A. V. GRANATO
Department of Physics, University of Illinois, Urbana, Illinois
(Received 23 March 1964; revised manuscript received 9 October 1964)

Measurements were made of the release of stored energy during the annealing from 15 to 80°K of copper irradiated with 11-MeV deuterons. A differential thermometry technique using two closely matched specimens, one of which was irradiated, was employed. Loss corrections and heat capacities were determined for the range of temperature of annealing. Two irradiations, with different total damage dose, and subsequent anneals were made. Good definition of the peak substructure in stage I was obtained. The magnitude of the energy released is consistent with the interstitial-vacancy annihilation mechanism of radiation damage annealing. The energy-to-resistivity ratio found is in disagreement with the ratios obtained previously for neutron and electron damage. Assignments are obtained for the volume change, resistivity, and number of Frenkel pairs introduced in a damaged copper specimen for a given assumed value of the energy of a Frenkel pair. The results are compared with theory.

I. INTRODUCTION

THE primary purpose of the experiment described here was to decide whether or not the recombination of interstitials and vacancies is a possible mechanism for the recovery of radiation damage in deuteron-irradiated copper. Several other purposes were served at the same time. One such was to develop a reliable method of counting the number of interstitials and vacancies introduced by radiation damage. The energy of a Frenkel pair can be estimated much more accurately than other commonly used properties, such as resistivity. In addition, it was desired to complete the program begun at Illinois of measuring many physical properties on the same system. Previously, the resistivity,[1] lattice parameter,[2] and length change[3] of deuteron-irradiated copper had been measured. Also, a number of new results became available while the experiment was in preparation, and the experimental design was adjusted to give information concerning some of the new questions. For example, the kinetics of the recovery were studied by making measurements at two different total dose levels.

The first measurements of radiation damage at helium temperatures were made by Cooper, Koehler, and Marx[1] (hereafter referred to as CKM), who measured the resistivity introduced by 12-MeV deuteron irradiation in copper, silver and gold at 10°K, together with the

* This research was supported in part by the U. S. Atomic Energy Commission.
† Present address: U. S. Steel Corporation, Applied Research Laboratory, Monoreville, Pennsylvania. Taken in part from a thesis submitted in partial fulfillment of the requirements for the degree of Doctor of Philosophy at the University of Illinois.

[1] H. G. Cooper, J. S. Koehler, and J. W. Marx, Phys. Rev. **97**, 599 (1955).
[2] R. O. Simmons and R. W. Balluffi, Phys. Rev. **109**, 1142 (1958).
[3] R. Vook and C. Wert, Phys. Rev. **109**, 1529 (1958).

recovery of this resistivity as the specimen was annealed to higher temperatures. They discovered a conspicuous annealing stage near 40°K, which has been termed stage I of the annealing spectrum. Subsequent measurements of the lattice parameter by Simmons and Balluffi (SB) and of length changes by Vook and Wert (VW) showed that all three quantities recovered by approximately the same relative amounts in the same annealing temperature regions. This was interpreted to mean that interstitials and vacancies were recombining by mutual annihilation in the recovery process, since otherwise the three properties would not be expected to anneal together. This viewpoint was supported by earlier theoretical calculations[4–6] which predicted that the damage should consist largely of equal numbers of interstitials and vacancies. This model predicts the amount of stored energy that should be released in the annealing process to be in the range of 3–5 eV per Frenkel pair or about 4–7 cal/g per $\mu\Omega$cm.

However, Blewitt, Coltman, Holmes, and Noggle[7] found that the energy released after neutron irradiation of copper was less than 0.9 cal/g per $\mu\Omega$cm of resistivity which anneals. Actually, no energy release was observed but this figure represented the estimated limit of error. This value was much lower than expected and led to doubts as to whether or not interstitial-vacancy mutual annihilation could be the recovery mechanism. Further, since the annealing observed in deuteron-irradiated copper is in some ways similar to that found in neutron damage, the doubt applied as well to the deuteron results. Other recovery mechanisms had been postulated (for example, the reordering of disturbed regions of the lattice which were initially disordered by displacement spikes[8]), but these offered less definite predictions about the energy release to be expected upon annealing.

While the present experiment to measure the stored-energy release after deuteron bombardment was in preparation, a number of new important results became available. More accurate measurements were obtained by the Oak Ridge group showing a definite energy release of 1.6 cal/g per $\mu\Omega$cm.[9] However, this was still too small to allow for a Frenkel pair annihilation mechanism interpretation. Further measurements by Magnuson, Palmer and Koehler (MPK)[10] after deuteron irradiation disclosed substructure in stage I of the annealing spectrum of copper. These were interpreted as the recombination of close-pairs (interstitial-vacancy pairs close enough together to exert an attraction on one another) with interstitials moving freely in the higher temperature range of stage I. More detailed measurements of stage I annealing by Corbett, Smith and Walker (CSW)[11] revealed that there are five substages (labeled I_A, I_B, I_C, I_D, and I_E by CSW in order of increasing temperature). In addition, CSW studied the concentration dependence of the peak structure and were able to show from this that peaks I_A, I_B, and I_C had the characteristics expected of close-pair recovery, while peaks I_D and I_E could be shown to be associated with a defect which is capable of freely migrating through the lattice. Following Huntington's[12] calculations, the defect is identified as an interstitial atom. Peak I_D was interpreted as the correlated recombination of an interstitial with its own vacancy, and the concentration-dependent peak I_E as uncorrelated long-range interstitial recombination.

Meechan and Sosin[13] measured the stored-energy released in stage I after 1.2-MeV electron irradiation. They reported an energy-to-resistivity ratio of 5.4 cal/g per $\mu\Omega$cm, which is not inconsistent with a vacancy-interstitial annihilation mechanism. The measurements were not sensitive enough to detect the peak substructure. More will be said about this later.

A preliminary report on some of the results found after deuteron bombardment has already been given.[14] The energy-to-resistivity ratio found in this work is 6.4 cal/g per $\mu\Omega$cm, so that no "energy paradox" exists for deuteron damage. Subsequently, Blewitt[15] has argued that corrections can be applied to their neutron data which would raise their value to a level which is no longer inconsistent with the Frenkel pair annihilation mechanism. Blewitt argues that since an observable energy release was found only in the 35–45°K range, only the resistivity annealing in this region, and not all the resistivity annealing in stage I, should be used. This increases the energy-resistivity ratio to 2.5 cal/g per $\mu\Omega$cm. Blewitt further argues that, in fact, only $\frac{2}{3}$ of the resistance recovered between 35 and 45°K should be used in the calculation since the rest corresponds to the background resistivity observed in the rest of stage I for which no energy release is observed. The final result obtained in this way is 3.8 cal/g per $\mu\Omega$cm. This leaves open the question as to why the method does not detect the energy release corresponding to the rest (and biggest part) of the resistivity change in stage I.

There still remains a substantial discrepancy between this result for neutron damage and the result found here for deuteron bombardment. It is therefore felt worthwhile to describe the experimental procedure used here

[4] F. Seitz, Discussions Faraday Soc. **5**, 271 (1959).
[5] W. Harrison and F. Seitz, Phys. Rev. **98**, 1530 (1955).
[6] J. Neufeld and W. S. Snyder, Phys. Rev. **99**, 1326 (1955).
[7] T. H. Blewitt, R. R. Coltman, D. K. Holmes, and T. S. Noggle, in *Dislocations and Mechanical Properties of Crystals*, edited by J. C. Fisher, W. G. Johnston, R. Thomson and T. Vreeland, Jr. (John Wiley & Sons, Inc., New York, 1956), p. 603.
[8] J. A. Brinkman, J. Appl. Phys. **25**, 962 (1954); Am. J. Phys. **24**, 246 (1956).
[9] T. H. Blewitt, R. R. Coltman, and C. E. Klabunde, Phys. Rev. Letters **3**, 132 (1959).
[10] G. D. Magnuson, W. Palmer, and J. S. Koehler, Phys. Rev. **109**, 1990 (1958).
[11] J. W. Corbett, R. B. Smith, and R. M. Walker, Phys. Rev. **114**, 1452, 1460 (1959).
[12] H. B. Huntington, Phys. Rev. **91**, 1092 (1953).
[13] C. J. Meechan and A. Sosin, Phys. Rev. **113**, 422 (1959).
[14] A. V. Granato and T. G. Nilan, Phys. Rev. Letters **6**, 171 (1961).
[15] T. H. Blewitt, *Radiation Damage in Solids*, edited by D. S. Billington (Academic Press Inc., New York, 1962), p. 630.

in some detail. Also, the method used is new and promises to be useful for a number of applications.

In the following section the calorimeter design and experimental technique are described. It is shown, for example, that it is not possible, in principle, to obtain an effect in which losses are negligible for the conditions of the experiment.

There follows a section in which the results are described. The results are grouped into two classifications: integrated and differential. By integrated results, we refer to total changes in stage I of the recovery, such as the total energy released, or energy-to-resistivity ratio. By differential results, we refer to the amounts of recovery per unit temperature interval. A number of conclusions follow from an analysis of the differential results, and these are discussed separately in a second article.

II. CALORIMETER DESIGN

The difficulties of the experiment have been emphasized by previous workers.[9,13] They are mostly connected with the fact that the amount of energy released is small. In the present experiments, this is between 1/20 and 1/50 calorie. Furthermore, this energy is released gradually, so that one needs a sensitive calorimeter to detect the effect. In addition, one would like sensitivity sufficient not only to measure the total amount released, but also to measure the peak structure. Although the amount of energy released is small, the specific heat is also small in stage I, so that one might expect to get a temperature increase of the order of a degree in a thermally "isolated" specimen when the defects anneal out. This is sufficiently large to measure accurately in a differential calorimeter. The difficulty is in obtaining a thermally "isolated" specimen.

In order to design a sufficiently sensitive calorimeter it is necessary to look more closely into the meaning "isolated." We consider two specimens, with external heat input rates $\dot{H}_1$ and $\dot{H}_2$, but specimen (1) contains stored energy. Then the rate of increase of the internal energy of each is given by

$$m_1c_1(T_1)(dT_1/dt)=\dot{E}(T_1,dT_1/dt)+\dot{H}_1-P_1(T_1)T_1,$$

and (1)

$$m_2c_2(T_2)(dT_2/dt)=\dot{H}_2-P_2(T_2)T_2,$$

where m_1 is the mass of specimen 1, etc., c is the specific heat, T is the temperature, $\dot{E}$ is the rate at which stored energy is released, and PT is the heat loss rate. We may appreciate the main effects in a simple way by considering only a highly idealized system. The more complete analysis needed for processing the actual data is given in Appendix II.

We assume first of all that the system is perfectly symmetric. That is, the materials are the same, with exactly the same geometry, the external heat input rate, and the loss rate are the same for each specimen. We further assume that the specific heat and the loss-rate coefficient P are temperature-independent. Then, letting $\delta T=T_1-T_2$, one has

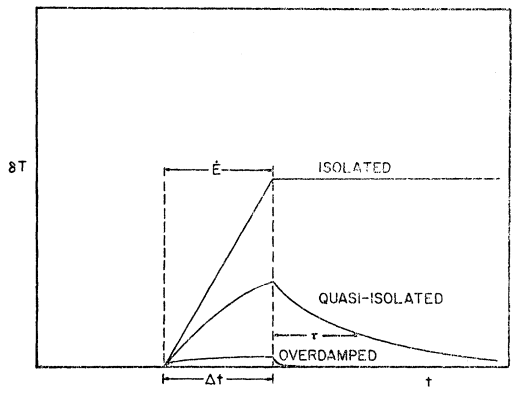

FIG. 1. Schematic diagram defining thermally isolated differential system in an ideal case. The temperature difference between two specimens δT is shown as a function of time. A constant differential heat input $\dot{E}$ is applied during the interval Δt.

$$mc(d\delta T/dt)=\dot{E}-P\delta T. \quad (2)$$

Then, for the case where $\dot{E}$ is zero everywhere except for a region of width Δt, the difference temperature is a simple exponential, as shown in Fig. 1.

$$\delta T=(\dot{E}/P)(1-\exp(-t/\tau)), \quad \text{with} \quad \tau=mc/P. \quad (3)$$

The necessary conditions for the design of the calorimeter can be discussed in terms of this simple diagram. If the loss-rate coefficient $P=0$, the maximum temperature difference $\delta T=(\dot{E}/mc)\Delta t$ is achieved. This is called the thermally isolated case. If the losses are such that the time constant τ is of the order of the time interval Δt, the system will be termed "quasi-isolated." If the time constant τ is much less than Δt, the heat leaks away as fast as it is released and the difference temperature achieved is only $\delta T=\dot{E}/P=(\delta T)_I(\tau/\Delta t)$, where $(\delta T)_I$ is the temperature difference which would be obtained for an isolated system.

If the specific heat is not constant, then a similar effect occurs even if there are no losses. To see this simply, we consider a case in which there are no heat losses ($P=0$), but $c(T+\delta T)=c(T)+(dc/dT)\delta T+\cdots$. We then obtain

$$mc(d/dt)(\delta T)=\dot{E}-[m(dc/dT)(dT/dt)]\delta T, \quad (4)$$

so that there is an effective loss coefficient (P_{eff}) given by

$$P_{\text{eff}}=m(dc/dT)(dT/dt). \quad (5)$$

This is easily understood physically. If one specimen gets warmer than the other as a result of stored-energy release, then its specific heat is higher if the specific heat increases with temperature. If then, both specimens are given the same further increment of heat, the

temperature of the hotter specimen increases less than that of the cooler specimen since its specific heat is higher. Thus δT decreases, and the effect is similar to that obtained for a system of two specimens with constant specific heat but finite loss coefficient. We may make a crude estimate of the influence of this effect by considering the system in a region where the specific heat increases with the cube of the temperature. If $c=c_0T^3$, then $dc/dT=3c/T$, $P_{\text{eff}}=3mc\beta/T$ (where $\beta=dT/dt$), and $\tau=T/3\beta$. For the heating rate used in the present experiment, $\beta\approx 2$ deg/min. The main peak to be measured is located at about $T=40°$K and is about 10 degrees wide ($\Delta t\approx 5$ min). We thus find $\tau\approx 7$ min at 40°K. This means that even for a system with no losses, the "isolated" state cannot be achieved with a differential system at this heating rate. In fact, these figures imply that if the quasi-isolated state is to be obtained with $\tau=\Delta t$, then the loss coefficient P must be held to less than 6 μcal/deg sec.

There are a number of ways of maximizing the temperature difference δT. First, the specific stored energy E can be maximized by using a long bombardment. However, there is a limitation set on this by the requirement that the stored energy should be less than than the specific heat. Otherwise the specimen would become thermally unstable and its temperature would increase spontaneously (Wigner effect). At high temperatures, this is not a severe limitation, but at low temperatures, the specific heat is small and the effect becomes important at relatively low doses, This is discussed in more detail in the second article. In fact, it was necessary to operate at damage levels much lower than those which had been used in previous deuteron experiments. For the second run, the dose was about 20 times smaller than the usual. The damage which annealed in stage I for the second run in the present experiments was within 10% of that used in the electron damage measurements of Meechan and Sosin[13] and the neutron damage measurements of Blewitt, Coltman and Klabunde[9] as judged on the basis of the resistivity which anneals in stage I.

A second method of maximizing δT is simply to anneal very fast, making Δt small. The limitations here are those of preserving near-equilibirum conditions in the specimen and also the necessity of having sufficient time available to collect required data. In the present experiment, a heating rate of about 2°K/min was achieved. A third method of maximizing δT is to maximize the mass of the specimen. However, the specimen is limited in area by the deuteron beam and in thickness by the deuteron range. Specimens of about $\frac{1}{2}$ g were used (but less than half of the specimen area was irradiated).

Finally, the only remaining possibility is that of making the heat-loss coefficient P, a minimum. There are three contributions to the heat-loss coefficient: heat conduction through the (thermocouple and heater) wires to the specimens (P_w), heat conduction through the residual gases (P_G) surrounding the specimen, and thermal radiation (P_R). We consider each in turn.

A commonly used thermocouple system has been copper-Constantan. Each specimen has two thermocouples (one for absolute and one for differential temperature measurements) and two wires to the heaters on the specimen. For two copper wires of 4-mil diam and 10 cm length, the expected heat-loss coefficient would be 50 μcal/deg sec as compared with the allowable 6μcal/deg sec. We conclude that pure metals are unsuitable as thermocouple wires and that alloy systems are to be preferred. A Chromel-Advance system was used in this work.

The radiation loss coefficient (given by $P_R=4Ae\sigma T^3$) contributes only at the highest temperature. For $A=5$ cm^2, $e=1/10$, $\sigma=5\times10^{-5}$ (cgs), $T=80°$K, one obtains $P_R=1.2$ μcal/deg sec. It is interesting to note that the time constant $\tau=mc/P$ is limited in materials which have a specific heat which is cubic in temperature, even if conduction losses are completely eliminated. Since both c and P are cubic in temperature in such a case, a constant time constant is obtained.

The heat-loss conduction through the residual gas depends upon the pressure of the gas. For pressures greater than that for which the mean free path is less than a characteristic length of the apparatus (about 3×10^{-3} mm Hg in the present case) the heat loss is independent of pressure. In the present experiment, it was necessary to have a reproducible heat loss, since the heat loss must be measured and taken into account in the experiment. Wire conduction losses are reproducible, but gas conduction losses are not, since it is difficult to avoid small fluctuations in pressures at low levels. In order to guarantee reproducibility, the pressure was maintained at a level (less than 10^{-5} mm Hg) such that the gas conduction was a small percentage of the wire conduction.

In summary, these considerations show that for the design of a calorimeter to meet the needs of the present experiment, a number of conditions have to be met. The thermocouples should be of alloy material, the pressure should be maintained below 10^{-5} mm Hg, and the loss rate should be reproducible and measurable. Also, since heaters are attached to the specimen, the specific heat of the specimen is different from that of pure copper and also needs to be measured. There is little use in using thermopiles, since the extra signal is lost through the added heat loss. Also, it is seen that there is little point in reducing the heat losses below the levels already described for two reasons. First, in the quasi-isolated state, the signal is already near the maximum achievable. A decrease in losses by several orders of magnitude would not further increase the signal an appreciable amount. Secondly, although the wire conduction losses could be further reduced, the limitation would then become gas conduction loss, which is difficult to make reproducible. Also, it is necessary to have heat leaks which are large enough so that the specimens could cool down

to the base temperature in a reasonable period of time after an anneal following irradiation to allow a background run to be made. The complete analysis, taking into account asymmetries and higher orders in difference temperature, is given in Appendix II. Asymmetries can be taken into account experimentally by making "background" runs, which are heating curves taken for the system when no stored energy is released. Based upon the design considerations, the calorimeter described in the following section was constructed.

III. APPARATUS

The apparatus is schematically depicted in Fig. 2. The specimens were 0.55 g Cu foils, $0.75\times1.0\times5\times10^{-3}$ in. in size. These were formed by cold reduction of ASR high-purity copper, followed by stress-relief annealing in vacuum. Resistivity ratios were obtained on adjacent strips annealed at the same time for an estimate of purity. The ratio of room temperature to liquid-helium temperature resistivity found was 900. For 2 $\mu\Omega$cm/percent of impurities, this would indicate an impurity concentration of 1×10^{-5}, i.e., the Cu was of "five nines purity." One of the specimens (A) is shown edge-on in annealing position. The specimens were enclosed in a massive copper chamber (B) machined from electrolytic tough pitch copper which was in good thermal contact with a liquid-helium reservoir. During the irradiations and anneals this chamber was maintained at liquid-helium temperature. The pressure in the experimental volume was less than 10^{-5} mm Hg during all anneals. The thermal contact between the chamber and the reservoir was a pressure contact improved by coating the opposing faces with Micro-Circuits Company SC-12 Ag paint.[16] Because of the necessity of dissipating a large amount of heat, a sizeable liquid-helium reservoir was needed. For this purpose a 30 liter liquid-helium cryostat was fabricated by Superior Air Products Company, following the basic cryostat design used in earlier deuteron experiments.[17] The specimen chamber was surrounded by a shield (C) which was maintained at liquid-nitrogen temperature. The deuteron beam entered the specimen chamber after passing through three Al foils which served, in turn, to isolate the cryostat from the cyclotron vacuum and to cover beam apertures in the nitrogen-temperature shield and specimen chamber. These foils had a total thickness of 1.9×10^{-3} in. and absorbed 0.7 MeV of the 11-MeV deuteron energy. The specimen to be irradiated was firmly clamped against the helium temperature wall of the chamber by block (D). The clamped area was well removed from the area to be irradiated. The effects of this deformation upon the recovery in the irradiated volume were estimated to be negligible. The effective thermal conductivity of this clamp was 0.2 W/°K,

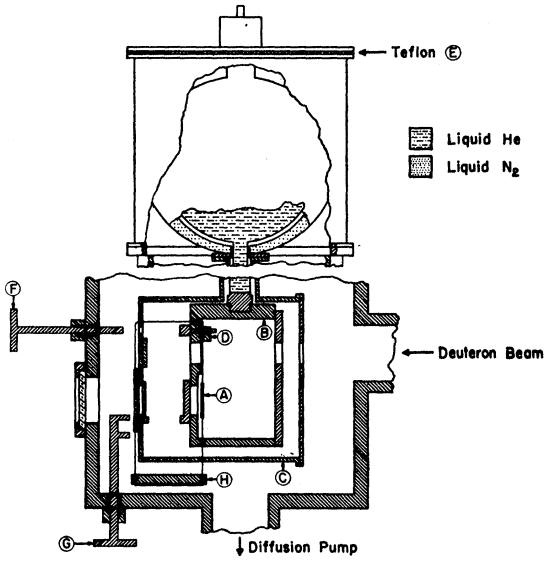

FIG. 2. Schematic drawing of cryostat and experimental volume. Specimen A shown in annealing position.

which prevented the specimen temperature from rising above 10°K during irradiation. The average deuteron dissipated 7 MeV in the specimen. In order that the remaining deuteron energy not be dissipated at helium temperature, the deuterons which passed through the specimen passed from the specimen chamber through another Al foil and were finally stopped in a Cu block on the nitrogen shield. The cryogenic fluid reservoirs and the chamber and shield attached to them were insulated from the rest of the apparatus by the Teflon gasket (E), and served as a Faraday cage to accumulate the charge of the deuteron beam. The charge was bled off through an Eldorado Electronics integrator which provided a charge output to a Sedeco counter in 7.5 μC units for the measure of the integrated flux and a target current output for the cyclotron operator's information.

When the desired flux has been accumulated, the clamp was loosened by moving rod (F) in to engage the screw holding the clamp and freeing it. Rod (G) was then rotated to grasp a runner on the face of the nitrogen shield to which the specimen was attached by nylon threads. Counterweight (H) insured the threads remaining taut at all times. By moving the runner up to a predetermined location, the irradiated specimen was lowered into a position symmetrical with the unirradiated specimen. These specimen manipulators entered the apparatus through vacuum-tight double O-ring sliding seals. A window in the sump and doors on the shield and chamber permitted a check on specimen alignment when necessary.

In the annealing position, both specimens were under closely matched thermal conditions. They were suspended within the chamber by nylon threads of low thermal conductivity. To each specimen were also

[16] Recommended by S. L. Quimby.
[17] D. E. Mapother and F. E. L. Witt, Rev. Sci. Instr. 26, 843 (1955).

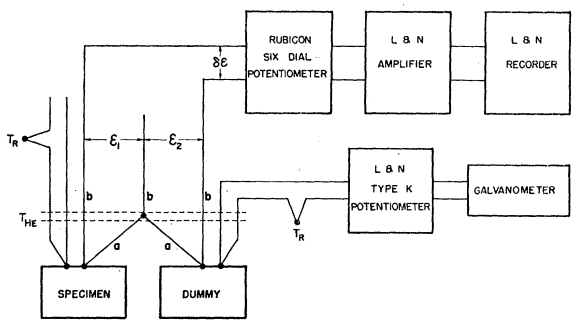

FIG. 3. Thermocouple circuitry. Wires a: Advance; wires b: Chromel P.

attached two thermocouple junctions and two heater wires. The thermocouples will be discussed in a later section. The specimens were annealed simultaneously by the heaters bonded to each specimen. These heaters were formed from 3-in. lengths of 1-mil Nichrome wire having a room-temperature resistance of 160 Ω and bonded to the specimen in an area which was not irradiated by a film of G.E. 7031 high-thermal conductivity varnish. Advance wire, 4×10^{-3} in. diam, was used for current leads to the heaters to minimize the loss of heat from the specimens.

The heat capacity of the specimens increased by twentyfold over the temperature range of interest. This necessitated a programing of the heat input in order to obtain a fairly constant rate of anneal. A voltage across the heaters increasing linearly with time, hence giving a quadratic increase in power input, approximated the temperature dependence of the heat capacity and produced an annealing rate of approximately 2°K/min. The high thermal diffusivity of Cu in this temperature range, of the order of 50 cm^2/sec, assured that the temperature distribution over the specimen was uniform to within 0.1°K.

The thermocouple circuitry is shown in Fig. 3. Advance-Chromel P thermocouples were used for all junctions. The wire sizes were 5 mil for the Advance (a) and 4 mil for the Chromel P (b). These alloys proved to have very uniform thermoelectric properties and to be insensitive in these properties to moderately heavy working. The prime advantage of these alloys was their low-thermal conductivity, limiting the heat losses from the specimens. All leads from the specimens were lagged at helium temperature. In addition to providing a sink for the heat conducted from room temperature, this lagging insured a reproducible heat sink for the heat flow from the specimens during annealing. This permitted a unique heat-loss determination to be made which was applicable for all runs that were made on a particular set of specimens, with the proviso that the system pressure be the same. As shown in Fig. 3, the midpoint of the Advance differential thermocouple link between specimen and dummy formed a junction with a Chromel lead, the junction and leads being lagged at helium temperature. The purpose of this treatment of the junction was twofold. First of all, with this arrangement, a separate calibration of each differential thermocouple junction was made against liquid-helium temperature. The particulars of this calibration are given in Appendix I. Secondly, the lagging of the differential link at the midpoint thermally isolated each specimen from the other. Thus, the differential thermocouple could be calibrated solely in terms of the temperature of the differential junctions since the Thomson emfs of the half-differential link were the same in the calibration and runs.

To insure the best thermal contact, the midpoint junction was soldered to the liquid-helium reservoir. As a consequence of this electrical connection, the reference junctions for the thermocouples used to measure the absolute temperature of the specimens could not be connected to the same reservoir. Such connections would short-out the measuring junctions since both differential and absolute junctions were soft soldered to the foils. Therefore, these reference junctions were immersed in a thermostatically controlled oil bath at 55°C capable of maintaining a constant temperature to ±0.01°C. All these thermocouples were calibrated at one time *in situ* against two platinum resistance thermometers calibrated by the National Bureau of Standards, and the two reference baths. Each resistance thermometer took the position of one of the specimens. The temperature differences developed over all leads for a given junction temperature were the same in both the thermocouple calibration and the experimental run. The output of the differential thermocouple when both specimens were in the annealed condition, $\delta_0\epsilon(T)$, was a measure of the thermal asymmetry of the specimens. With proper attention to maintaining initial conditions, successive background anneals showed that the temperature difference between specimens could be kept to within 0.2°K and reproducible to ±0.01°K over the range of absolute specimen temperature of 15–80°K. This emf, $\delta_0\epsilon$, was determined following each experimental anneal and applied as a background correction to the run data.

The thermocouple wires were brought out of the apparatus through serum cap seals and attached to shielded copper microphone cables, Belden No. 8440, at massive Cu lagging blocks within an enclosure which minimized transient air current disturbances of the emf. The high electrical resistance of these thermocouple alloys precluded a direct run to the measuring apparatus. The same cabling was used in both calibration and experimental runs. The differential emf was measured by a Rubicon 6-dial potentiometer which was always within ±2μV of the balance. The unbalanced potential was amplified by a Leeds and Northrup microvolt dc amplifier, and continuously recorded on a Leeds and Northrup AZAR strip-chart recorder. The amplifier and recorder combination gave a sensitivity of 0.5 μV/in. on the chart. Due to the small magnitude

of the unbalanced emf, the recorder was linear in emf calibration for deflection on either side of the potentiometer balance point.

It was not possible to record the absolute emf due to feedback that was found to exist when two recorders were used. This did not pose any great problem since the dummy emf was a monotonically decreasing function of temperature during the anneal and could be manually measured to the accuracy desired by a Leeds and Northrup Type K potentiometer.

The equilibrium base temperature of the specimens in annealing position was about 16°K, the temperature depending critically upon specimen positioning. This base temperature, above that of the liquid-helium temperature of the chamber, was due to thermal radiation from the door of the chamber which was above the chamber temperature. Due to a disparity in the heat leaks, the dummy specimen had a lower base temperature than the irradiated specimen. This small difference could be used to advantage insofar as it permitted the undamaged specimen to be heated separately until the difference temperature was zero at which time the irradiated specimen heater was switched on. In this way, a consistent criteron for the start of the annealing was obtained, i.e., zero-difference temperature, and this was in no way influenced by the level of damage as it would be if the irradiated specimen was initially at a lower temperature.

A Bodine K-2 electric motor geared down to 1/40 rpm drove a carbon composition potentiometer across a 6 V dc potential. Both heaters, with their meters and current controls, were paralleled across this increasing potential. It took approximately 30 min to anneal from 15 to 80°K.

The heat capacities of the specimens had to be determined, for they were thermal composites of the Cu specimens, solder, heaters, and their bonding agent. Although this excess material added only about 5% to the total mass of the specimens, the heat capacity was increased by about 40%. This is understandable if the effective Debye θ of the excess material is about half that of copper, since at low temperatures the heat capacity is approximately inversely proportional to the cube of the Debye θ. It was expensive in several ways to have the heater attached to the specimen. Most particularly, this meant that less of the specimen could be irradiated, since the heater with its bonding agent had to be shielded from the deuteron beam. However, the advantage of this arrangement was that the heaters delivered a measurable and reproducible power to the specimens, and could be used to pretest the apparatus by putting in a false-stored energy. It was felt that having this demonstrable check on the accuracy of the technique and the method of correcting for losses more than offset the disadvantages so incurred. The final arrangement of the specimen as seen from the incoming deuteron beam is shown in Fig. 4.

The often used method of measuring the latent heat

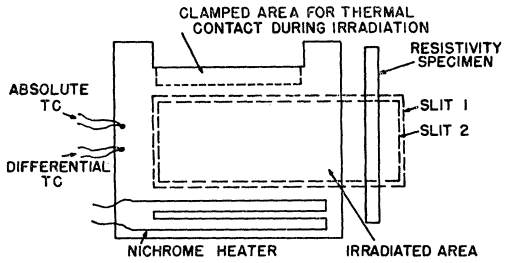

FIG. 4. Schematic diagram showing irradiated specimen and attachments.

during some phase transformation at a fixed temperature was judged to be unsuitable. In such a case the energy is released all at one temperature, whereas the kind of test needed was one in which energy is released continuously over a range of temperatures. The check was made by changing one heater current by set amounts during an annealing run, prior to irradiation. These dynamic power input changes were known to an estimated accuracy of ±5%. The total differential energy input was 46.6 mcal/g. The result of the analysis gave an "energy release" of 48.5 mcal/g, a difference of 1.9 mcal/g or an error of 4.1%. This is within the estimated accuracy of the measured input. No power changes were made above 45°K. In the temperature region above 55°K, the differential heat-loss correction is a maximum, hence any error in the correction scheme should be enhanced. The measurements showed the "energy release" to be zero in this region to within ±0.1 mcal/g°K. The scatter was uniformly distributed about the line of zero release. The check on the method and scheme of analysis was therefore excellent.

Following Overhauser,[18] Coltman *et al.*,[19] and Meechan and Sosin,[13] the specific heat was assumed to change a negligible amount on irradiation. Hence, the determination of heat capacities prior to the experimental runs sufficed for the analysis. These determinations were made *in situ* by a modification of the cooling curve method. The differential heat leak, pertinent to the analysis, was determined from the same data as the heat capacities, These determinations are described in Appendix II. The importance of the specific-heat correction is shown in Fig. 5, wherein the first-order loss-correction coefficients used in the final analysis are plotted. In the temperature region of prime interest, 30–45°K, the specific heat correction is seen to be about 3 times as large as the conduction heat-leak correction. The experimental heat capacity and hence the derivative was not a simple function of temperature due to the specimens being a composite of several materials and this is obvious in the plot of the specific heat correction.

The experimental data were obtained in the form of

[18] A. W. Overhauser, Phys. Rev. **94**, 1551 (1954).
[19] R. R. Coltman, T. H. Blewitt, and T. S. Noggle, Rev. Sci. Instr. **28**, 365 (1957).

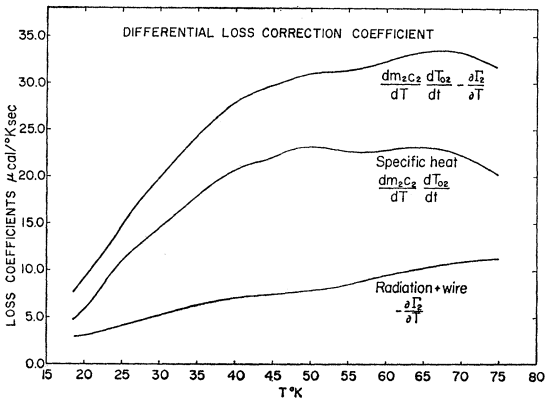

FIG. 5. Differential loss coefficients used in the stored-energy analysis. The net correction coefficient is the sum of the specific heat and conduction loss coefficients. The notation is that used in the Appendix.

recordings of the difference thermocouple emf versus time for the stored-energy release run and the background runs. Two successive background runs were made to check the reproducibility. These data were then reduced by the method described in Appendix II.

Alignment and Irradiation

The irradiation was done at the University of Illinois cyclotron using 11.0±0.1-MeV deuterons. As described in the previous section, thermocouple junctions, heaters, and supporting threads were attached to the foils. Any changes in the properties of these elements on irradiation would place in doubt the accuracy of the measurement, hence care had to be taken to protect them from the deuteron beam. As a result, only 39.3% of the stored-energy specimen was irradiated.

Prior to the bombardment, with the specimens protected, determinations of the deuteron beam location and uniformity were made with a motor-driven grid of probes placed just before the defining aperture. When the cyclotron was in stable operation, a selector switch sampled the pickup from each probe. This was amplified by the Eldorado Integrator current circuit and recorded. The spread of the beam was adjusted by means of a quadrupole lens placed between the cryostat and the cyclotron, approximately 10 ft from the defining aperture. The optimum conditions produced a beam that was uniform to within 3% over the aperture. However, the uniformity of the beam was sensitive to the quadrupole-lens adjustment, and there is some evidence that the beam was not uniform during the runs. This is discussed more fully later in the section in which the probable error of the flux measurement is discussed.

Measurement of the deuteron flux required that only the number of incident deuterons be counted. Any secondary electron ejected from the aperture foil on the nitrogen shield, due to the incident deuterons, which did not return to the shield, would result in a spurious deuteron count. A retarding electrode, concentric with the beam and facing this foil, was kept at 50 V below ground potential and served to return all secondaries to the Faraday cage.

In order to make use of the results of the other deuteron experiments and to compare the present results with this earlier work, it was necessary to normalize all results to a standard integrated flux and deuteron energy in the specimen.

Vook and Wert[3] and Simmons and Balluffi[2] both found the damage production to be linear with integrated flux to within experimental error for fluxes up to 6×10^{16} d/cm^2. Simmons and Balluffi in the same paper also reported that damage was inversely proportional to the deuteron energy in the specimen. Since the earlier deuteron experiments, improved range-energy calculations for charged particles in Cu and Al have been made, namely those of Sternheimer[20] for proton energies above 2 MeV and Allison and Warshaw[21] for proton energies below 2 MeV.

In the light of the new range-energy data, the average of the inverse of the deuteron energy in the specimens was recalculated for the previous deuteron experiments, in the same manner as described here. The computation was carried out in the following fashion.

Let $f(T)=(dT/d\xi')$ the stopping power where T is the deuteron energy and $\xi'=\rho x$, the distance traversed in g/cm^2. The deuteron energy T after penetration of ξ g/cm^2 of material is obtained by integration of the following equation from the incident energy to energy T.

$$\xi'=\int_{T\text{incid}}^{T}[dT/f(T)]\,. \tag{6}$$

This integration was done graphically on a plot of the inverse of the stopping power versus T for sufficient values of T to provide a suitable plot of T^{-1} versus ξ. The average of the inverse of the deuteron energy was obtained from the graphical integration of

$$(1/T)_{\text{av}}=\xi^{-1}\int_0^{\xi}[T(\xi')]^{-1}d\xi'\,, \tag{7}$$

where ξ was the total thickness of the material.

Taking into account the aforementioned proportionalities, the results of all experiments were then normalized to an integrated flux of 10^{17} d/cm^2 and a reciprocal of the average inverse deuteron energy in the specimen of 10 MeV. Whenever deuteron energy in the specimen is mentioned in this paper, reference is made to the reciprocal of the average inverse deuteron energy in the specimen.

Since the entire specimen was not irradiated, a choice

[20] R. M. Sternheimer, Phys. Rev. **115**, 137 (1959).
[21] S. K. Allison and S. D. Warshaw, Rev. Mod. Phys. **25**, 779 (1953); also *American Institute Physics Handbook*, edited by D. E. Gray (McGraw-Hill Book Company, Inc., New York, 1957), Sec. 8, p. 35.

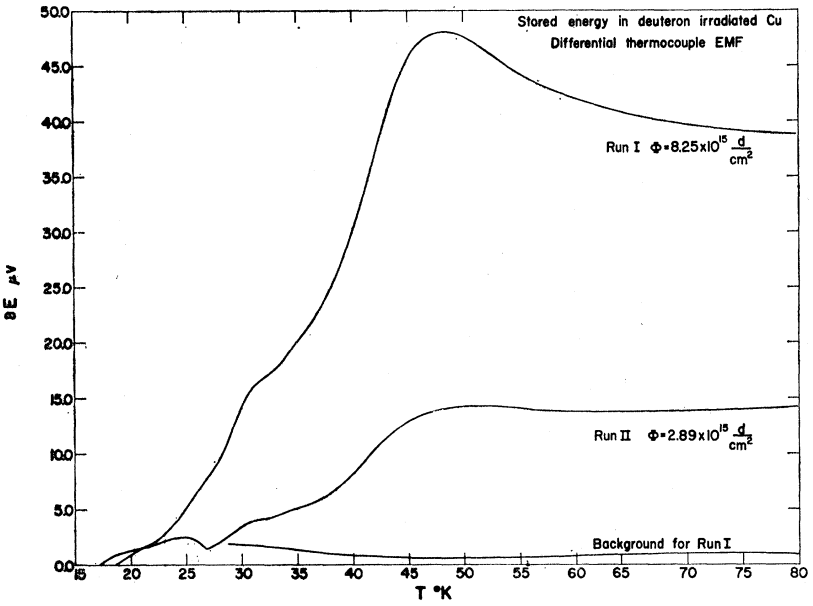

FIG. 6. Differential thermocouple emf in μV for stored-energy runs I and II and a background run after run I vs irradiated specimen temperature. The portion of the background run below 29°K has been omitted for clarity.

must be made on deciding whether an effective integrated flux is considered or an effective mass of specimen. In the latter instance this would mean considering the effective mass to be the irradiated volume. Both procedures give the same results under the normalization to 10^{17} (d/cm^2) and 10 MeV. The choice has been to report the measured energy release per total mass of Cu in the specimen for irradiation by an effective integrated flux of 39.3% of the measured integrated flux.

Two irradiations and subsequent anneals were made using the same specimens. After each stored-energy anneal, two anneals over the same temperature range as the energy-release anneal were made to obtain the background correction and check its reproducibility. These background anneals were made without disturbing either the specimens or the heater controls. Analysis of the cooling curves made between these anneals showed that one loss correction could be used for all runs. Between irradiations the specimens were annealed to room temperature, the system opened and the specimen reclamped in position for irradiation.

IV. RESULTS

The first irradiation was to an effective integrated flux of 8.25×10^{15} d/cm^2, the second to an effective integrated flux of 2.89×10^{15} d/cm^2. The initial data,

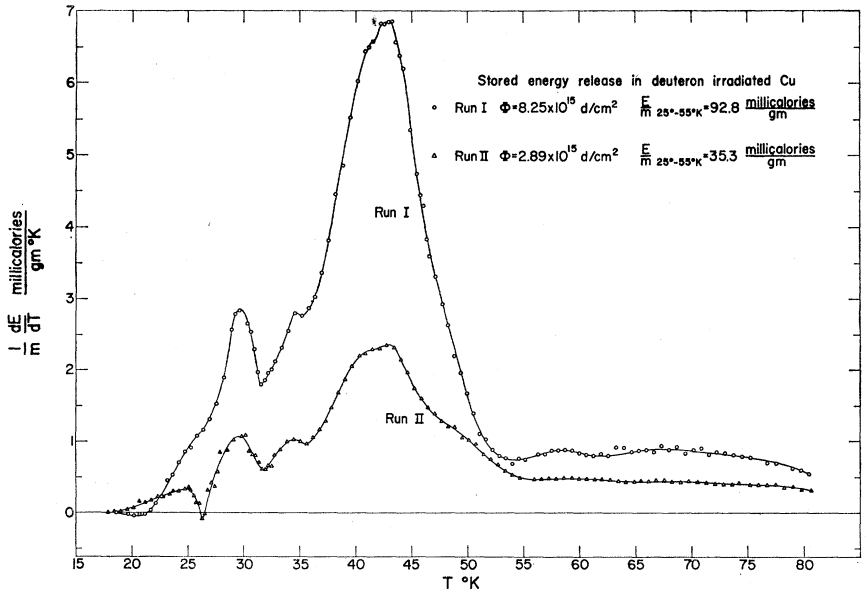

FIG. 7. Stored-energy release per gram °K in runs I and II vs irradiated specimen temperature for the noted effective integrated deuteron fluxes.

the differential thermocouple emf, $\delta_r\epsilon$ in μV, are shown in Fig. 6 as a function of the irradiated specimen temperature. In addition to the two run curves, a representative background is shown for comparison. The maximum difference emf was 47 μV for run I and 15 μV for run II. The background magnitude did not exceed 2.4 μV on any run. The shielding of cables and apparatus proved quite satisfactory, keeping the average peak-to-peak noise amplitude to 0.05 μV. The recorder charts were a plot of $\delta\epsilon$ versus time, effectively 10 by 15 ft plots of the data. The first data reduction, the time derivative of the difference emf, was made directly on these charts.

The results of the final computation using Eq. (38) of Appendix II are shown in Fig. 7. The results are given as the energy released per gram $-$°K as a function of specimen temperature. Good peak shapes are obtained because the data are essentially continuous. The only previous measurements showing the peak structure in stage I were by MPK and CSW using resistivity measurements. It is difficult to obtain good peak-shape definition with resistivity measurements because of the necessity either of returning to helium temperature to measure the residual resistivity after each measurement or of taking into account deviations from Mathiesson's rule for measurements made at annealing temperatures. For many of the peaks, only 4 or 5 points have been available to define the peak shape with resistivity measurements. Stored-energy measurements, which are essentially continuous data taken in a single run, have an advantage over resistivity measurements in this regard. The data of MPK have been reanalyzed by Herschbach,[22] who obtained more detailed definition of peak shape. However, the peaks referred to here are peaks in the activation energy spectrum rather than peaks in the annealing temperature scale. The distinction between these is discussed in the second article. More recently Tesk, Jones, and Kaufman[23] and Sosin and Bauer[24] have made measurements of electrical resistivity recovery following electron bombardment at higher energies and have also obtained more detailed definition of peak shape with evidence for further structure.

Three main peaks are observed in both runs, centered at 29.6, 34.5, and 42.5°K. The agreement in temperature of the peak positions is approximately 0.1°K for the two runs. Following Corbett, Smith, and Walker the the peak at 29.6°K is called I_B, that at 34.5°K, I_C, and the large peak at 42.5°K, I_D. The "bump" on the high-temperature side of I_D will be referred to as I_E. Peaks I_B and I_C maintain approximately the same relative height in both runs. However, the height of I_D relative to I_B and I_C is greater in run I than in run II. Peak I_D does not shift position in temperature with increased irradiation but does show that more defects recombine at this temperature the higher the dose. Peak I_E is more pronounced in run II and is almost absorbed into I_D in run I. This peak shifts to lower temperatures with the higher dose and is considered to be the same uncorrelated recovery discussed by CSW. Peak I_E was not seen in previous deuteron experiments, which were all at such high doses that peak I_E would be expected to be unresolvable from peak I_D. Peak I_A was not observed because the annealing started at too high a temperature. Thus, the structure observed by MPK and CSW with resistivity measurements has been reproduced. In addition, a new substructure is observed in peak I_D. This may be seen near the top of peak I_D, and although it is not very pronounced, the definition of the peak shape is good enough so that it is definitely detected, and also reproduced in run II.

The relative peak heights are the same as that found by MPK for deuteron bombardment, but different from that found by CSW for electron bombardment. The annealing found above 55°K is larger than that found by MPK.

The conditions before annealing were not identical for runs I and II. First of all, the irradiated specimen equilibrated at different temperatures in each run after lowering to annealing position, 18.6°K in run I and 17.2°K in run II. Secondly, there was a 3-h interval from the time the specimen was lowered into position until the start of the anneal in run I, and only 1 h in the case of run II. These factors contributed to the differences evident between the runs below 25°K. The lower limit of the analysis was therefore set at 25°K since any isothermal annealing at the base temperatures should have small effect upon the annealing above this temperature.

Although the data below 25°K are not used in the analysis, it is easy to show that the two curves are in agreement below 25°K when the annealing at the base temperature is taken into account. A calculation was made of the curve shape to be expected for constant-heating-rate annealing of a specimen which has been standing at the base temperature of 18.6 and 17.2°K for 3 h and 1 h, respectively. The expected curve shape (assuming a constant activation energy spectrum) for dE/dT would be zero for a few degrees, followed by an increase, again taking a few degrees to develop, to the full value which would have been found if no annealing at constant temperature had taken place. This is what is observed, and a comparison of observed and expected results indicates that the annealing curve should be regarded as approximately constant in the interval between about 25–22°K. Between 25 and 27°K, there was a difficulty with the type K potentiometer used for measuring the temperature of the dummy specimen. The potentiometer is of the type having a slide wire on a drum. At 25°K, it was necessary to change scales and unwind the entire drum. It is believed that the friction

[22] K. Herschbach, Phys. Rev. **130**, 554 (1963).
[23] J. A. Tesk, E. C. Jones, Jr., and J. W. Kauffman, Phys. Rev. **133**, A288 (1964).
[24] A. Sosin and W. Bauer, Bull. Am. Phys. Soc. **9**, 283 (1964).

on the slide wire caused an error in the emf reading, thus accounting for the discrepancy in the curves for runs I and II in this temperature interval. The details of the curves in this region should be ignored. Analysis of the cooling curves following each run showed that the differential heat leaks were the same as those computed during the heat-capacity measurements.

The energy released in the temperature range from 25–55°K was obtained by integration of the curves in Fig. 7 over the temperature interval. In run I there was a release of 92.8 mcal/g and in run II 35.3 mcal/g. The deuteron energy in the specimen was the same for both runs, 7.04 MeV. The energy released when normalized to the conditions of 10-MeV deuteron energy and 10^{17} d/cm^2 integrated flux are: for run I $E/m_{25-55°K}=0.79$ cal/g; for run II $E/m_{25-55°K}=0.86$ cal per g. The average of the two runs is $E/m_{25-55°K}=0.83\pm0.04$ cal per g. The deviation about the average is 5%. This normalization to a standard flux also shows that the production of stored energy is linear with integrated flux to within 5%. The error in the energy measurement itself is judged to be ±5%, based upon the pseudo run test described earlier and on the agreement between run I and run II. However, evidence for a systematic error in the measurement of the flux has been obtained. The resistivity of a specimen placed alongside the stored-energy specimen was measured for run II. An attempt to do so also for run I failed. The resistance increase was found to be 40% less than that expected from the data of CKM. If this were a true reading corresponding to a uniform flux, the resulting energy to resistivity ratio would be unreasonably high. It is preferable to regard this as evidence that the deuteron beam intensity was not uniform, but low near this end, despite the fact that the probe measurements mentioned earlier made before the run suggested no inhomogeneity of this magnitude. This then implies that the effective flux over the specimen used for the stored-energy measurements might have been as much as 10% higher than the average flux as measured by the total charge passing through the first slit area. As we have no way of determining the amount, we prefer to report the flux as the measured amount with a systematic error of from +0 to −20%. Combining this with the ±5% for the energy measurement, we obtain for the measured ratio of energy-to-flux the value $\Delta E/\Delta\varphi=0.83\times10^{-17}$ cal/g per d/cm^2 (+5%, −20%).

The ratios of the energy released to the changes in other physical properties in stage I recovery after deuteron irradiation are of particular interest. In order to derive these ratios, one must assume that the percent recovery releasing the stored energy measured in this experiment is the same as the percent recovery in the other deuteron experiments during stage I. Due to the differences in annealing rates, the maximum rate of recovery does not occur at the same temperature in all experiments. The annealing rate in the present work of approximately 2°K/min was 30 to 40 times the rate of anneal in the other deuteron experiments which will be referred to, hence the prominent recovery took place at a higher temperature.

All the other deuteron experiments[2,3,10] have consistently shown a stage I recovery of 55–60%. Since the starting temperature is higher in this work, the recovery between 25–55°K is considered to be 55%. CKM[1] reported the initial resistivity increment in Cu upon deuteron irradiation to be 2.3×10^{-7} Ωcm/10^{17} (d/cm^2). In the CKM irradiation, the deuteron energy in the specimen was 9.27 MeV. Therefore, on normalization to 10 MeV, the resistivity increment will be 0.21 μΩ cm/10^{17} (d/cm^2). VW found the macroscopic change in length per unit length for 10^{17} d/cm^2 irradiation to be 3.8×10^{-4}. The lattice parameter increment found by SB was the same to within the error of the experiments. The deuteron energy in the specimen in the VW experiment was 8.65 MeV which leads to a volume increment of 9.8×10^{-4} per 10^{17} d/cm^2 at 10 MeV. For 55% recovery from these values, one finds the energy released per μΩcm recovery to be 7.1 (cal/g-μΩ cm). The probable error of this result is the probable error of $\Delta E/\Delta\varphi$(+5%, −25%), combined with the (unknown) probable error of the CKM resistivity result. Thus the measured value of $\Delta E/\Delta\rho$ is 7.1 cal/g per μΩ cm, whereas a perhaps more useful value for calculations is 6.4 cal/g per μΩ cm. Then the energy released per atomic volume change is 3.7 eV per atomic volume change. If one assumes that the recombination of each Frenkel pair releases 5 eV of stored energy, then the dilatation per Frenkel pair is 1.35 atomic volumes per F.p. and the resistivity/percent of Frenkel pairs is 2.9 μΩcm per % F.p.

There is an independent method of obtaining a value for $\Delta E/\Delta\rho$ with the present data for which the flux of particles need not be known. The temperature at which peak I_E occurs depends upon the concentration of defects and the annealing rate. Thus, the energy associated with peak I_E can be compared with the CSW value of the resistivity which anneals in peak I_E for equivalent concentrations of defects. In the second paper, the method of separating peak I_E from I_D for the deuteron data is described, and this comparison is discussed more fully. The result is $\Delta E/\Delta\rho=5.6$ cal/g per μΩcm±25%. The probable error quoted represents only the error associated with the difficulty of locating the peak temperature accurately in the resistivity data for peak I_E when only a few data points are available for defining the peak shape. If account is taken of the probable error in the measured energy and of the activation energy of peak I_E, then the probable error of $\Delta E/\Delta\rho$ as determined by this method will be larger than 25%. The value found by the first method of comparing only deuteron experiments is contained within the (wider) limits found by the second method. We therefore adopt the deuteron result of $\Delta E/\Delta\rho=6.4$ cal/g per μΩcm±15% as the most probable value, keeping in mind that ±15% does not include any error in the resistivity measurement of CKM.

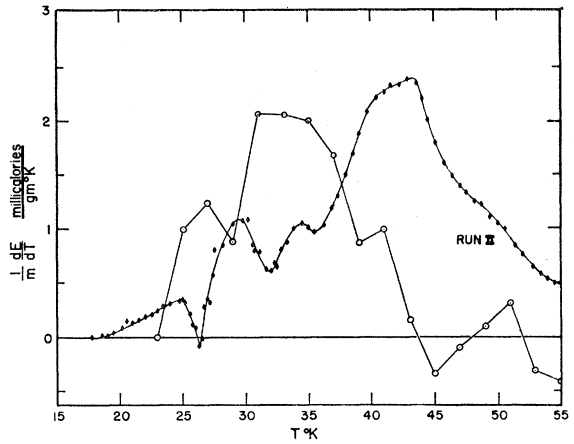

FIG. 8. A comparison of the stored-energy data for deuteron damage (run II) with that for electron damage. Based on the resistivity changes in stage I, the area under the electron dose curve should be about 8% greater than that under the deuteron dose curve. Although the values of the integrated energy release for stage I are in fair agreement, there is disagreement on a peak-by-peak basis.

V. DISCUSSION

In this section, the results will be compared with those found by other measurements, and with theoretical estimates. Meechan and Sosin have reported a value of $\Delta E/\Delta\rho = 5.4 \pm 0.8$ cal/g per $\mu\Omega$cm for the energy-to-resistivity ratio after 1.2-MeV electron bombardment. This result would not appear to be in serious disagreement with that given here. However, an examination of the results shows that this is too superficial a comparison. Figure 8 shows the electron data plotted on the same scale as the deuteron data (run II). Based on the resistivity changes in stage I the area under the electron-dose curve should be about 8% greater than that under the deuteron-dose curve. It may easily be seen that the results disagree in detail. In fact, for peaks I_B and I_C, the energy-to-resistivity ratio for the electron results is about twice that for the deuteron results, while for peaks I_D and I_E, this ratio is about $3\frac{1}{2}$ times less than that for the deuteron results. In the electron experiment, the heating rate was about twice that for the deuteron experiment so that the equivalent peak positions for the electron results should be expected to be at higher temperatures than those found for the deuteron experiment. This correction has not been made in Fig. 8 and this effect would tend to increase the discrepancy. Alternatively, it might be supposed that the discrepancy arises from a systematic error in thermocouple calibration beyond the three degree uncertainty suggested by Meechan and Sosin. If this error were about 10°, then the curves would resemble each other. In such a case, however, the calculated energy-to-resistivity ratio would be invalid because the values used for the specific heat and resistance changes in the calculation would be in error. In this temperature region, the specific heat changes rapidly with temperature, and a 10° increase corresponds to a specific heat increase of about a factor of 2. This factor of 2 could, perhaps, be accommodated by changing the correction scheme used by Sosin and Meechan. As they themselves pointed out, a large correction has been applied to the data. The final values of total energy released are not measured values but values corrected upward by a factor increasing with temperature. The correction factor used for temperatures of 30°K, 40°K, and 50°K are about 3, 4.5, and 19, respectively. This correction factor was determined by assuming that the heat-loss correction is proportional to the difference temperature and that no recovery occurs between 43°K and 45°K. According to the deuteron results, this is where the maximum recovery rate should occur. Thus, it appears to us that the energy-to-resistivity ratio reported for electron damage is not sufficiently well established.

As has already been noted, the energy-to-resistivity result for neutron damage obtained by Blewitt and his co-workers at Oak Ridge differs from that given here (3.8 against 6.4 cal/g per $\mu\Omega$cm). As with the Illinois experiments, the Oak Ridge group has measured stored energy, resistivity and length changes resulting from the same type of bombardment.[25] A summary of the results is given in Table I. Notable points about the Oak Ridge measurements are the fact that the length-change-to-resistivity ratio was determined on the same specimen, and that a second measurement (on a B^{10}-doped copper specimen) gave an energy-to-resistivity ratio (4.0 cal/g per $\mu\Omega$ cm) similar to that found for pure copper. In the latter case, both energy and resistivity were measured on the same specimen and a large effect was obtained. However, the full resistivity change

TABLE I. Comparison of deuteron stage I radiation damage results with neutron results and with theory.

	10-MeV deuterons	Oak Ridge reactor	Theoretical
$\Delta E/\Delta\rho$(cal/g)/($\mu\Omega$ cm)	$6.4 \pm 15\%$[a,b,c]	3.8[f]	
$(\Delta l/l)/\Delta\rho(\mu\Omega\text{ cm})^{-1}$	1.6×10^{-3} [c,d]	1.25×10^{-3}[g]	
$(\Delta a/a)/\Delta\rho(\mu\Omega\text{ cm})^{-1}$	1.4×10^{-3}[c,e]		
			3.1[h]
$(\Delta E)/(\Delta V/V)$(eV)	3.7[b,d,e]	2.8[b,g]	2.6[i]
			2.0[j]
$\Delta E/\Delta\phi$	0.75×10^{-17} (cal/g)/(d/cm^2) $\pm 15\%$[b]		4.1×10^{-17} (cal/g)/(d/cm^2)[k]

[a] The $\pm 15\%$ error does not include the (unknown) error of the resistivity measurement.
[b] Data of present work used.
[c] Data of Cooper, Koehler and Marx (Ref. 1) used.
[d] Data of Vook and Wert (Ref. 3) used.
[e] Data of Simmons and Balluffi (Ref. 2) used.
[f] Data of Blewitt, Coltman and Klabunde, as reinterpreted by Blewitt (Ref. 15).
[g] Data of Blewitt, Coltman and Klabunde (Ref. 25).
[h] A. Seeger and E. Mann (Ref. 26).
[i] L. Tewordt (Ref. 27).
[j] R. A. Johnson and E. Brown (Ref. 28). Johnson and Brown regard their value as a lower limit since electronic redistribution energy is neglected.
[k] F. Seitz and J. S. Koehler (Ref. 29). In calculating this value, an energy per Frenkel pair of 5.0 eV has been used.

[25] T. H. Blewitt, R. R. Coltman, and C. E. Klabunde, in *Proceedings of the International Conference on Crystal Lattice Defects*, J. Phys. Soc. Japan 18, Suppl. III, 283, 288 (1963).

in stage I was used in this case, and not a fraction of it as was done in the case of pure copper discussed previously.

Blewitt has suggested[15] that the discrepancy in the energy-to-resistivity ratio between deuteron and neutron results may be due to an error in the CKM resistivity measurements, since they were taken some time ago. Although this measurement has never been repeated, there are two reasons for not being optimistic about possible modifications in this direction. First, as Blewitt has pointed out, the length-change-to-resistivity ratio measured in the neutron experiment is in fair agreement with the lattice parameter to resistivity measurement in the deuteron experiments. If the resistivity change is altered to bring the energy-to-resistivity into agreement, then the length change-to-resistivity measurement would disagree. Secondly, although the CKM resistivity-to-flux ratio for copper has not been checked, the corresponding ratio CKM measured at the same time for gold has been recently checked by Herschbach.[22] Herschbach found that if damage is assumed to vary inversely as the energy of the bombarding particle, then his value for the resistivity-to-flux ratio was less than that of CKM by only 10%.

Theoretical values of the energy and volume change for a Frenkel pair have been given by Seeger and Mann,[26] Tewordt,[27] and Johnson and Brown.[28] These differ somewhat in values of energy and volume change, but one would expect that the ratio of energy-to-volume change should be more accurate than either quantity alone, since the same model is used for both and some errors should tend to cancel. The values are listed in Table I, where it may be seen that the neutron results agree fairly well with the theoretical values. However, according to the deuteron results, the theories underestimate the ratio of energy to volume change for a Frenkel pair.

The energy-to-deuteron flux ratio may be used to estimate the amount of damage produced by 10-MeV deuterons. This may be compared with a theoretical figure, if the energy per Frenkel pair is known. Assuming 5 eV for the latter and using the method of Seitz and Koehler[29] for the calculation, one obtains the results shown in the last line of Table I. The observed damage is 5.5 times less than the calculated damage rate.

Again, assuming 5 eV/F.p. and using the deuteron data, one finds that the fractional volume change per Frenkel pair is $\Delta V/V$ per F.p.$=1.35$. This agrees with the value computed by Tewordt[27] who, however, computes 3.5 eV for the energy/F.p. The value computed from Table I using the deuteron data for the resistivity is $\Delta\rho=2.9$ $\mu\Omega$ cm/1% F.p. which agrees well with Blatt's[30] calculated value of 2.7 μcm/1% F.p.

[26] A. Seeger and E. Mann, Phys. Chem. Solids **12**, 326 (1960).
[27] L. Tewordt, Phys. Rev. **109**, 61 (1958).
[28] R. A. Johnson and E. Brown, Phys. Rev. **127**, 446 (1962).
[29] F. Seitz and J. S. Koehler, *Advances in Solid State Physics* (Academic Press Inc., New York, 1956), Vol. 2, p. 305.
[30] F. J. Blatt, Phys. Rev. **99**, 1708 (1955).

VI. CONCLUSIONS

(1) The experiment demonstrates that stored energy is a useful property for measurement of defect annealing, and its use has advantages over some more commonly used techniques. It is more sensitive than length change or lattice parameter. It also has advantages over resistivity measurements. These are (a) that energy is a more fundamental property and is better known theoretically than resistivity, and (b) that essentially continuous annealing data can be obtained for stored energy.

(2) The magnitude of the energy released is large enough to allow for the vacancy-interstitial annihilation mechanism of radiation-damage annealing.

(3) Peaks I_B, I_C, I_D, and I_E of stage I annealing have been observed, with good definition of peak shapes. Peak I_D has a substructure. Peak I_E has not been observed in previous deuteron experiments all of which were done at higher dose levels.

(4) The relative peak heights are in good agreement with those found by resistivity measurements for deuteron damage by Palmer, Magnuson, and Koehler, and are in qualitative agreement with, but differ quantitatively from, those found for electron damage by Corbett, Smith, and Walker.

(5) The measured energy-to-flux ratio for 10-MeV deuterons is 0.83×10^{-17} cal/g per deuteron/cm^2 ($+5\%$, -25%), meaning that the most probable value is 0.75×10^{-17} cal/g per deuteron/cm$^2\pm15\%$. The corresponding energy to resistivity ratio $\Delta E/\Delta\rho$ is 6.4 cal/g per $\mu\Omega$ cm$\pm15\%$. This is 10% less than the result given in a preliminary report,[14] owing to a 10% systematic error suspected in the flux measurement.

(6) Using the results listed in (5) above, and previous measurements of resistivity, length, and lattice parameter changes for deuteron irradiation, experimental values for the ratios of energy-to-resistivity, length-to-resistivity, and energy-to-volume changes are found. If the energy per Frenkel pair is assumed to be 5.0 eV, the resulting fractional volume change per F.p. is 1.35 and resistivity change per 1% of F.p. is 2.9 $\mu\Omega$cm. An independent method of computing $\Delta E/\Delta\rho$ using data of this experiment and resistivity measurements for electron data gives a result with a larger probable error, but which is not in disagreement with that found from the deuteron data. The results for $\Delta E/\Delta\rho$ are in disagreement with those found from neutron and electron experiments. According to the deuteron results, theory underestimates somewhat the energy-to-volume ratio for a Frenkel pair and overestimates by a factor of 5.5 the damage production rate for 10-MeV deuterons (assuming 5 eV/F.p.).

ACKNOWLEDGMENTS

The authors wish to express their thanks to Professor J. S. Koehler for his continuous advice and help in carrying through the experiment. The help of R. Seigel,

Professor R. Coleman, Dr. M. Garfinkel, Professor R. O. Simmons, and Dr. J. Bredt is gratefully acknowledged. They thank the members of the Nuclear Radiation Laboratory under Professor J. S. Allen, Professor S. Chatterjee, and L. Ernest and the Liquid Helium Service under Professor D. E. Mapother for their generous assistance. Also, they are indebted to F. Witt for much useful advice and help, particularly on the construction of the calorimeter.

APPENDIX I. THERMOMETRY

This Appendix will be concerned with the thermocouple calibration and the method of obtaining the differential temperature from the measured differential thermocouple emf.

The thermocouples were calibrated after being permanently wired in the cryostat. In order that the irradiated specimen could be raised and lowered, approximately 3 cm of the thermocouples at the junction end were not fastened rigidly in place. Those thermocouples on the dummy specimen were fastened in the same way to equalize the heat leaks. The mode of wiring allowed the junctions to be transferred easily from the calibrating blocks to the specimens without disturbing the securely fastened portions of the thermocouples.

In the calibration, the specimens were replaced by copper cylinders enclosing platinum resistance thermometers and wound with Nichrome heaters. The silver-soldered thermocouple junctions were soft-soldered to projections on these cylinders, and the cylinders were so placed that the junctions were in the same position in the calorimeter chamber as they would be during the annealing.

The calibration blocks were then raised in temperature in approximately 3°K increments from liquid-helium temperature to 87°K. At each increment, once the elements had reached a constant temperature, all junctions were calibrated against the Pt thermometers.

Following calibration, the junctions were removed from the calibration blocks and soft-soldered to the specimens.

In order to avoid a possible change in the thermoelectric properties of the thermocouple junctions on irradiation, the junctions were attached at the edge of the specimens, removed from the region to be irradiated. The thermal diffusivity of Cu in the temperature range of this experiment is of the order of 50 cm²/sec. Calculations of the temperature distribution in the specimen, with this diffusivity and the heater power input used, showed that the temperature would be uniform over the specimen to within approximately 0.1°K. The maximum rate of stored-energy release was about 30 μW, two orders of magnitude less than the heater power input. Since the computation showed the temperature variation to be proportional to the power input, for the geometry of the specimen used, the distribution of the temperature over the specimen due to the stored-energy release was well within the error of the absolute temperature measurement which we take to be of the order of ± 0.1°K.

The prime consideration is the obtaining of the differential temperature in terms of the differential emf. Following the convention of the text of this paper, the subscript 1 refers to the irradiated specimen and the subscript 2 to the unirradiated, dummy specimen. Referring to the differential thermocouple circuit as shown in Fig. 2, the junction at the midpoint of the differential link was in contact with the liquid-helium reservoir and permitted separate calibrations to be made of both specimen junctions against the liquid-helium temperature reference: Hence there were two calibrations, $T_1(\epsilon)$ and $T_2(\epsilon)$. In general, these calibrations will not be equal for a given emf but rather will be related by

$$T_1(\epsilon)=T_2(\epsilon)+\Delta T(\epsilon), \tag{8}$$

where $\Delta T(\epsilon)$ is the temperature difference when the separate thermocouples produce the same emf. This ΔT is due to differences in the thermoelectric properties.

During the experiment there will be temperatures $T_1(\epsilon_1)$ and $T_2(\epsilon_2)$, where ϵ_1 is the emf of junction 1 and ϵ_2 the emf of junction 2. These temperatures are related by

$$T_1(\epsilon_1)=T_2(\epsilon_2)+\delta_a T. \tag{9}$$

The subscript a differentiates between background or run. The measured quantity will be the difference of the emf's, $\delta\epsilon$, defined as

$$\epsilon_1=\epsilon_2+\delta\epsilon. \tag{10}$$

Now consider $T_2(\epsilon_2)$. Using (10) one can write

$$T_2(\epsilon_2)=T_2(\epsilon_1-\delta\epsilon). \tag{11}$$

Expanding this expression about ϵ_1 in powers of $\delta\epsilon$, one obtains

$$T_2(\epsilon_2)=T_2(\epsilon_1)-(\partial T_2/\partial\epsilon)_{\epsilon_1}\delta\epsilon +1/2(\partial^2 T_2/\partial\epsilon^2)_{\epsilon_1}\delta^2\epsilon+\cdots. \tag{12}$$

From (8) one can write

$$T_2(\epsilon_1)=T_1(\epsilon_1)-\Delta T(\epsilon_1). \tag{13}$$

Therefore

$$T_2(\epsilon_2)=T_1(\epsilon_1)-\Delta T(\epsilon_1)-(\partial T_2/\partial\epsilon)_{\epsilon_1}\delta\epsilon +1/2(\partial^2 T_2/\partial\epsilon^2)_{\epsilon_1}\delta^2\epsilon+\cdots. \tag{14}$$

Now from (9) $T_2(\epsilon_2)-T_1(\epsilon_1)=-\delta_a T$. Therefore, letting

$$\tau_n=((-1)^{n+1}/n!)(\partial^n T_2/\partial\epsilon^n)_{\epsilon_1},$$

$$\delta_a T(\epsilon_1,\delta\epsilon)=\Delta T(\epsilon_1)+\sum_{n=1}^{\infty}\tau_n\delta_a{}^n\epsilon. \tag{15}$$

Since ϵ_1 corresponds to a unique T_1, $\delta_a T(\epsilon_1,\delta\epsilon)=\delta_a T(T_1,\delta\epsilon)$.

The thermal asymmetries of the specimens, which can be due to differences in heat capacities, heat leaks, and heater input, will be an additional source of temperature difference not due to stored energy and will be evident in an anneal prior to irradiation. This difference temperature is defined as the background difference temperature, $\delta_0 T$. In an anneal following irradiation, there will be a difference temperature $\delta_r T$ which will be the sum of the background difference temperature and an additional difference temperature due to the stored-energy release δT. Hence, at any point of this anneal there will be a temperature difference between specimens given by

$$\delta_r T(T_1)=\delta T(T_1)+\delta_0 T(T_1). \tag{16}$$

Therefore, the differential temperature due to the stored-energy release will be

$$\begin{aligned}\delta T(T_1)&=\delta_r T(T_1)-\delta_0 T(T_1)\\&=\Delta T(T_1)+\sum \tau_n \delta^n{}_r\epsilon-\Delta T(T_1)-\sum \tau_n \delta_0{}^n\epsilon\end{aligned} \tag{17}$$

or

$$\delta T(T_1)=\sum_{n=1}^{\infty} \tau_n(T_1)(\delta_r{}^n\epsilon-\delta_0{}^n\epsilon). \tag{18}$$

Therefore, the use of the background eliminates the asymmetry term in the thermocouple calibration. $\delta_r\epsilon$ is the difference emf measured during the first anneal following irradiation and $\delta_0\epsilon$ is the difference emf during the background anneal; both emfs measured when the irradiated specimen is at temperature T_1.

The derivatives in the expansion coefficients τ_n are obtained from the polynomial least-squares fit to the calibration data for the junction on the unirradiated specimen. The form of the analysis was such that this was the only junction out of the four measuring junctions for which a least-squares fit to the data was required. The cubic fit to the data was made using a modification of the Hayes and Vickers[31] orthogonal polynomial matrix method. The Crout[32] technique of matrix inversion permitted the computation to be carried through on a desk calculator.

The temperature-emf relationship is most easily expressed as $\epsilon(T)$. The cubic fit to the calibration data is given by

$$\begin{aligned}\epsilon=&-1.57-4.07(T/10^2)\\&+2086.17(T/10^2)^2-427.69(T/10^2)^3.\end{aligned} \tag{19}$$

The evaluation of this equation gives the emf in μV for T in °K, against a liquid-helium temperature reference. Between 12 and 80°K the average deviation of the calibration data from the least-squares curve was ± 0.3 μV. Over the temperature range of interest, 20–50°K, this deviation in emf corresponds to a temperature deviation of ± 0.03°K. As a check on the uniformity of the thermoelectric power of these Advance-Chromel P thermocouples, this same cubic equation was tried on the calibration data for one of the absolute temperature junctions which had been calibrated against the constant-temperature oil bath. The only adjustment in the equation was made in the constant term by evaluation of (19) at one temperature. The average deviation of the data from the equation so obtained was ± 1.1 μV or ± 1 part in 10^4 of the measured emf over the range 20–80°K. For a desired accuracy of ± 0.1°K in this range, this one equation could be used for all the thermocouples in this experiment providing the constant term was adjusted for each thermocouple at one temperature. In other words, for these thermocouples and to the accuracy required, $\Delta T(\epsilon)$ was essentially a constant.

[31] J. G. Hayes and T. Vickers, Phil. Mag. **42**, 1387 (1951).

[32] P. D. Crout, Trans. Am. Inst. Elect. Eng. **60**, 1235 (1941). A synthesis of these methods in Refs. 31 and 32 is printed in the following industrial report: E. B. Weinberger, Methods of Numerical Analysis, Vol. I and II, Computational Analysis Section, Report No. 1, Gulf Research and Development Company, 1953 (unpublished).

APPENDIX II. STORED-ENERGY-RELEASE ANALYSIS

Reduction of Experimental Data

The data have been obtained from a differential-thermocouple measurement of the temperature difference during annealing between irradiated and unirradiated specimens which were not perfectly balanced physically or thermally. The derivation of the analysis in the text of this paper adequately describes the method but does not take into account the existing asymmetries. In the derivation to follow, the only assumption made with regard to physical properties is that both the heat capacities and the heat losses are unchanged by irradiation, i.e., $mc(T_{r1})=mc(T_{01})=mc(T)$. Subscript 1 will refer to the irradiated specimen, subscript 2 to the unirradiated specimen as before. The subscript r will denote the run in which the stored energy is released and 0 will denote the background run when both specimens are in the annealed state. The heat capacity is spoken of rather than the specific heat since the heat capacity is the quantity directly measurable.

The equation of heat balance for the irradiated specimen in the stored-energy run is

$$m_1c_1(T_{r1})(dT_{r1}/dt)=dE/dt+\Gamma_1(T_{r1}) \tag{20}$$

and for the dummy specimen during the same anneal

$$m_2c_2(T_{r2})(dT_{,2}/dt)=\Gamma_2(T_{r2}), \tag{21}$$

where $mc(T)$ is the heat capacity; T is the absolute temperature of the specimen; $\Gamma(T)$ is the net heat input, due to the heater input less the heat leaks; and dE/dt is the time rate of release of stored energy.

As closely matched as the specimens were, it was impossible to eliminate all the asymmetries between them. These asymmetries are, in general, temperature-dependent.

Taking the asymmetries into account, the heat ca-

pacities and net heat-input terms, when both specimens are at identical temperatures, are related by

$$m_1c_1(T)=m_2c_2(T)+\Delta[mc(T)] \tag{22}$$

and

$$\Gamma_1(T)=\Gamma_2(T)+\Delta\Gamma(T). \tag{23}$$

The asymmetry terms are also to be considered as unaffected by irradiation.

In general, the difference temperature is defined by

$$T_{a1}=T_{a2}+\delta_aT, \tag{24}$$

where a can be either r or 0. The symbol δT, without subscript, will denote the difference temperature due solely to stored-energy release.

Therefore, for the stored-energy run, one has

$$T_{r2}=T_{r1}-\delta_rT. \tag{25}$$

Replacing T_{r2} in (21) by this expression gives

$$m_2c_2(T_{r1}-\delta_rT)[(dT_{r1}/dt)-(d\delta_rT/dt)] =\Gamma_2(T_{r1}-\delta_rT). \tag{26}$$

On expansion about T_{r1} in powers of δ_rT, one obtains

$$[m_2c_2(T_{r1})-\sum_{n=1}^{\infty}C_n\delta_r{}^nT](d/dt)(T_{r1}-\delta_rT) =\Gamma_2(T_{r1})-\sum_{n=1}^{\infty}g_n\delta_r{}^nT, \tag{27}$$

where

$$C_n=((-1)^{n+1}/n!)[(\partial^nm_2C_2)/(\partial T^n)]_{T_{r1}},$$
$$g_n=((-1)^{n+1}/n!)(\partial^n\Gamma_2/\partial T^n)_{T_{r1}}.$$

From (22) and (23) one can write

$$m_2c_2(T_1)=m_1c_1(T_1)-\Delta[mc(T_1)] \tag{28}$$

and

$$\Gamma_2(T_1)=\Gamma_1(T_1)-\Delta\Gamma(T_1). \tag{29}$$

On making these substitutions in (27) and replacing $m_1c_1(T_{r1})(dT_{r1}/dt)-\Gamma_1(T_1)$ by dE/dt as given in (20), one obtains

$$dE/dt=m_1c_1(T_1)(d/dt)\delta_rT +\sum\{C_n[(dT_{r1}/dt)-(d\delta_rT/dt)]-g_n\}\delta_r{}^nT +\Delta[mc(T_1)]\{(dT_{r1}/dt)-(d\delta_rT/dt)\}-\Delta\Gamma(T_1). \tag{30}$$

This expression for the time rate of stored-energy release still includes the asymmetry terms in the heat capacities and heat leaks. These are eliminated on the introduction of the background correction. The difference temperature at specimen temperature T_1 is related to the difference temperature due to the stored energy and that due to the asymmetries as follows:

$$\delta_rT(T_1)=\delta T(T_1)+\delta_0T(T_1). \tag{31}$$

Substituting this in (30) gives

$$dE/dt=m_1c_1(T_1)(d/dt)(\delta T+\delta_0T)+\sum\{C_n[(dT_{r1}/dt)-(d/dt)(\delta T+\delta_0T)]-g_n\}(\delta T+\delta_0T)^n +\Delta[mc(T_1)][(dT_{r1}/dt)-(d/dt)(\delta T+\delta_0T)]-\Delta\Gamma(T_1). \tag{32}$$

Now by definition $\delta T=0$ when $dE/dt=0$. Therefore, replacing the subscript r by subscript 0 in (32) and equating δT and dE/dt to zero, one obtains

$$\Delta\Gamma(T_1)=m_1c_1(T_1)(d/dt)\delta_0T+\sum\{C_n[(dT_{01}/dt)-(d/dt)\delta_0T]-g_n\}\delta_0{}^nT +\Delta[mc(T_1)][(dT_{01}/dt)-(d\delta_0T/dt)]. \tag{33}$$

Then (32) may be rewritten

$$dE/dt=m_1c_1(d/dt)\delta T+\sum\{C_n[(dT_{r1}/dt)-(d\delta T/dt)-(d\delta_0T/dt)]-g_n\} \times(\delta T+\delta_0T)^n-\sum\{C_n[(dT_{01}/dt)-(d\delta_0T/dt)]-g_n\}\delta_0{}^nT +\Delta[mc(T_1)][(dT_{r1}/dt)-(d\delta T/dt)]-\Delta[mc(T_1)](dT_{01}/dt). \tag{34}$$

Now

$$\delta_rT=T_{r1}-T_{r2}$$
$$\delta_0T=T_{01}-T_{02}$$

by (24). Then on subtraction and differentiation with respect to time

$$(d/dt)(\delta_rT-\delta_0T) =(dT_{r1}/dt)-(dT_{01}/dt)=(d\delta T/dt). \tag{35}$$

(dT_{02}/dt) and (dT_{r2}/dt) cancel since the dummy heating rate is the same in run and background, but from (31) $\delta T=\delta_rT-\delta_0T$. Therefore the asymmetry terms in the heat capacities cancel and in the first summation

$$(dT_{r1}/dt)-(d\delta T/dt)=(dT_{01}/dt),$$

but

$$(dT_{01}/dt)-(d\delta_0T/dt)=(dT_{02}/dt)$$

by (24). The final general form of the analysis is then

$$(dE/dt)=m_1c_1(T_1)(d/dt)\delta T +\sum'[C_n(dT_{02}/dt)-g_n](\delta T+\delta_0T)^n, \tag{36}$$

where $\sum'$ means terms in $\delta_0{}^nT$ are omitted. For $n=1$

we obtain

$$(dE/dt)=m_1c_1(T_1)(d/dt)\delta T + [(\partial m_2c_2/\partial T)_{T1}(dT_{02}/dt)-(\partial\Gamma_2/\partial T)_{T1}]\delta T. \quad (37)$$

This is the same in form as Eqs. (2) and (4) in the body of the paper where the derivation was made assuming a perfectly balanced system. For $n=2$

$$(dE/dt)=m_1c_1(T_1)(d\delta T/dt) + [(\partial m_2c_2/\partial T)_{T1}(dT_{02}/dt)-(\partial\Gamma_2/dT)_{T1}]\delta T - \tfrac{1}{2}[(\partial^2 m_2c_2/\partial T^2)_{T1}(dT_{02}/dt)-(\partial^2\Gamma_2/\partial T^2)_{T1}] \times(\delta^2T+2\delta T\delta_0T). \quad (38)$$

In Appendix I, δT is given by

$$\delta T=\sum \tau_n(\delta_r{}^n\epsilon-\delta_0{}^n\epsilon). \quad (39)$$

now $\delta T=(\partial T_2/\partial\epsilon)_{T1}(\delta_r\epsilon-\delta_0\epsilon)$ to first order and

$$(d\delta T/dt)=(\partial^2T_2/\partial\epsilon^2)_{T1}(\delta_r-\delta_0\epsilon)(d\epsilon/dt) + (\partial T_2/\partial\epsilon)_{T1}[(d\delta_r\epsilon/dt)-(d\delta_0\epsilon/dt)].$$

To first order in terms of the measured difference emf's the final result is

$$(dE/dt)=m_1c_1(T_1)\{(\partial T_2/\partial\epsilon)_{T_1}[(d\delta_r\epsilon/dt)-(d\delta_0\epsilon/dt)] + (\partial^2T_2/\partial\epsilon^2)_{T_1}(\delta_r\epsilon-\delta_0\epsilon)(d\epsilon/dt)\} + [(\partial m_2c_2/\partial T)_{T_1}(dT_{02}/dt)-(\partial\Gamma_2/\partial T)_{T_1}](\delta_r\epsilon-\delta_0\epsilon). \quad (40)$$

The desired quantity, the energy released per gram $-$°K, is obtained by dividing dE/dt by $m(dT_{r1}/dt)$.

The final result is independent of the asymmetries in Γ and mc to all orders. However, in the expansion for $n=2$, Eq. (38), the last term contains δ_0T. With reference to Eq. (15) of Appendix I, it is evident that this would introduce the thermocouple asymmetry term $\Delta T(T_1)$. As long as the two thermocouples are closely matched, maintaining ΔT small, the neglect of ΔT will be an error comparable with the next higher order term, hence the correction is good to second order. However, in the general case, a background correction is only complete in a computation to first order in difference temperature. The data of this experiment have been carried through second order.

There is a limitation imposed upon the differential method by this mode of analysis. It is clear from the form of Eq. (39) that the accuracy of the determination of δT is dependent on the convergence of the summation. For the thermocouples used, the ratio of the absolute values of successive derivatives, $|(\partial^{n+1}T/\partial\epsilon^{n+1})|:|(\partial^nT/\partial\epsilon^n)|$ was a linearly increasing function of n. The general term in (39) is $(1/n!)(\partial^nT/\partial\epsilon^n)\delta\epsilon^n$ and analysis shows that problems of convergence are serious for difference emf's in excess of 50 μV. Therefore run I represents close to the maximum allowable stored-energy content which can be handled by this mode of analysis for the experimental arrangement used. A higher level of stored energy could be accommodated by an increase in the loss rate which would lower the maximum difference emf.

The data reduction as described by Eq. (38) requires the determination of the heat capacities and differential loss coefficient as a function of temperature.

The heat capacities were measured using a modification of the cooling-curve method. Measurement of the resistance of the Nichrome heaters on the specimens showed that the resistance changed by only 2% from liquid-helium to liquid-nitrogen temperature. Therefore, using the average resistance between these two temperatures, an accurate measurement of heater current could give the heater power to within 1%.

The heat balance for a particular specimen on heating is given by

$$mc(T)(dT/dt)_h=\dot{Q}_{\text{in}}-\dot{Q}_{\text{out}}, \quad (41)$$

where $\dot{Q}_{\text{in}}$ is the heater power and $\dot{Q}_{\text{out}}$ is the heat loss through the heat leaks. The heat balance for the same specimen on cooling is

$$mc(T)(dT/dt)_c=-\dot{Q}_{\text{out}}. \quad (42)$$

Therefore

$$mc(T)(dT/dt)_h=\dot{Q}_{\text{in}}+mc(T)(dT/dt)_c \quad (43)$$

or

$$mc(T)=\dot{Q}_{\text{in}}/[(dT/dt)_h-(dT/dt)_c]. \quad (44)$$

$(dT/dt)_c$ is a negative quantity. Therefore, the denominator is nonzero. $\dot{Q}_{\text{in}}$ was determined from the heater resistance and current for a constant power input. The specimen temperature was recorded during heating and cooling and the computation of $mc(T)$ was made by use of the graphical derivatives of T_h and T_c at the specimen temperature, T.

The losses are introduced in the analysis by the partial derivative of the new power input with respect to temperature. Γ is given by

$$\Gamma=\dot{Q}_{\text{in}}(t)-\dot{Q}_{\text{out}}(T) \quad (45)$$

since $\dot{Q}_{\text{in}}$ is dependent explicitly only upon the drive-motor speed and applied voltage, not on the specimen temperature. Therefore,

$$(\partial\Gamma/\partial T)=-(d/dT)\dot{Q}_{\text{out}} \quad (46)$$

since $\dot{Q}_{\text{out}}$ is only a function of T. $\dot{Q}_{\text{out}}$ is already given by Eq. (42). Then the differential loss coefficient is

$$(\partial\Gamma/\partial T)_T=(d/dT)[mc(T)](dT/dt)_c. \quad (47)$$

This is also a negative quantity. All derivatives of these quantities were made graphically.